Tokai J Exp Clin Med., Vol. 30, No. 4, pp. 217-225, 2005

Ultrasonic Tissue Characterization of Photodamaged Skin by Scanning Acoustic Microscopy

Muneo MIYASAKA, Shingo SAKAI*, Ayumi KUSAKA*, Yoko ENDO*, Masaki KOBAYASHI*, Kazuto KOBAYASHI**, Naohiro HOZUMI*** and Ryuzaburo TANINO

Department of Plastic Surgery, Tokai University School of Medicine
**Basic Research Laboratory, Kanebo Cosmetics Inc.,*
***Research & Development Dept., Honda Electronics Co., Ltd.,*
****Dept. of Electrical & Electronic Engineering, Toyohashi University of Technology*

(Received August 26, 2005; Accepted October 21, 2005)

The aim of this study was to ultrasonically characterize photodamaged skin of the elderly at the microscopic level using scanning acoustic microscopy which showed two-dimentional distribution of sound speed in the skin section. We confirmed that the expression level of the elastin gene was increased in the preauricular skin (photodamaged area), compared with postauricular skin (photo-protected area). The expression level of the procollagen gene was also increased in the preauricular skin compared with postauricular skin. The preauricular skin showed higher sound speed in the papillary dermis (Grenz zone). The site of progressive solar elastosis showed a somewhat sound speed velocity than that of the Grenz zone. Immunohistochemical staining showed conserved deposition of collagen in the Grenz zone even in the more photodamaged preauricular skin. These results suggest that fibrosis in the Grenz zone compensates tissue strength with the progress of solar elastosis. The sound speed analysis of skin will provide important information on heterogeneous mechanical changes in the skin during the process of photoaging.

Key words: ultrasound, scanning acoustic microscopy, sound speed, collagen, photoaging, papillary dermis

Abbreviations: SC, stratum corneum; SAM, scanning acoustic microscope; EVG stain, elastica van Gieson's stain; MMP, matrix metalloproteinase.

INTRODUCTION

Photoaging is distinguished from intrinsic aging and shows some distinctive histological alterations including enlargement and dysplasia of keratinocytes in the epidermis, solar elastosis and a mixed inflammatory infiltrate in the dermis [1]. In particular, the dermal degeneration such as collagen [2, 3], elastin [4] and basal membrane [5] degeneration cause a decrease in the elasticity of skin [6], and promote the formation of wrinkles. So far, skin elasticity has been measured as a total physical property of multilayers such as the stratum corneum, keratinocyte layer and the dermis. Even in the dermis, there are the differences in thickness of collagen fibers [7] and the direction of elastic fibers [8] from the papillary dermis to the reticular dermis, but the contribution of localized changes in the physical properties of the dermis to the whole-skin elasticity during photoaging remains obscure. It is also important to clarify localized changes of physical properties in the skin in the formation of wrinkles.

A scanning acoustic microscope (SAM) system has been used to determine quantitatively the ultrasonic properties of tissue at the microscopic level. Two-

Muneo MIYASAKA, Department of Plastic and Reconstructive Surgery, Tokai University School of Medicine, Bohseidai, Isehara, Kanagawa 259-1193, Japan Tel: +81-463-93-1121 Fax: +81-463-93-7231 E-mail: miyasaka@is.icc.u-tokai.ac.jp

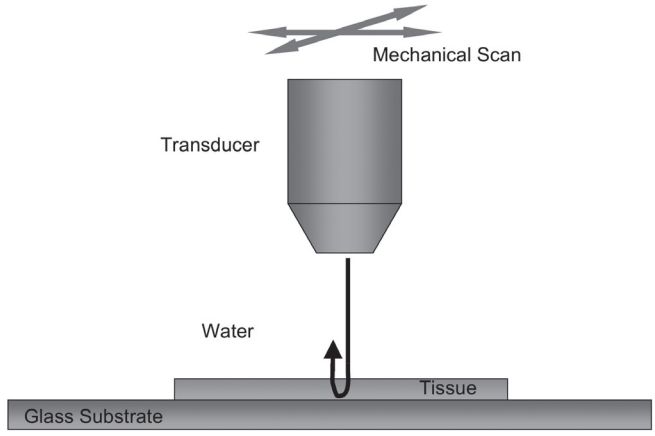

Fig. 1 Concept of ultrasonic microscopy for tissue characterization.

dimensional distribution of sound speed in microscopic sections can be obtained using the SAM system. The sound speed is considered to be mainly determined by the elastic property of tissue components on the assumption that biological tissue is fluid-like. In fact, Verdonk *et al*. [9] and Hoffmeister *et al*. [10] demonstrated that the velocity parallel to myocardial fibers was faster than the velocity perpendicular to the fibers. Saijo *et al*. reported high sound speed in fibrotic sites in the myocordium of patients with myocordial infarction [11]. However, measurement of the distribution of sound speed in the skin tissue using the SAM system has not been widely reported.

In this study, we ultrasonically characterize and compare a photodamaged skin section (preauricular area), and photo-protected skin (postauricular area but not buttock skin) using scanning acoustic microscopy, because regional differences in the structure of the skin have been reported [12].

MATERIALS AND METHODS

Biopsies

Eight Japanese volunteers (three men and five women; age range 66-83 years) were recruited for this study. Surgical biopsies were taken from both the preauricular skin and the postauricular skin of the same subject. The Tokai University Hospital Ethics Committee approved the study, and written consent was obtained from all subjects. Four healthy Caucasian female volunteers (age range 63-69 years) were also recruited. Punch biopsies (3 mm) were taken from the buttocks of each subject. Informed consent in writing was obtain from all subjects. Biopsy specimens were fixed in formalin, embedded in paraffin, sectioned to 10μm in thickness using a microtome, and deparaffinized for measurement using SAM.

Measurements By Scanning Acoustic Microscopy

Experimental setup

Figure 1 illustrates the concept of the ultrasonic microscope (HUM-1000, Honda Electronics Co., Ltd., Toyohashi, Japan) for tissue characterization. An acoustic wave is transmitted and received by the same transducer. Distilled water is used for the coupling medium between the specimen and the transducer. Reflections at both surfaces of the tissue are compared to measure the sound speed and thickness. Two-dimensional profiles of reflection intensity, thickness and sound speed can be obtained by mechanically scanning the transducer.

The transducer was 1.2 mm in aperture diameter, and 1.5 mm in focal length. Its nominal frequency range was 50-105 MHz (−6 dB), with a central frequency of 80 MHz. An acoustic wave with a wide frequency component was generated by applying the voltage pulse, and irradiated the substrate. The reflection was detected by the same transducer, and was introduced into the analog digital converter (ADC). The band limit and sampling rate were 500 MHz and 2.0 GS/s, respectively. In order to reduce random noise, eight of responses at the same point were averaged in the ADC before being introduced into the computer. The transducer

was mounted on an X-Y stage that was driven by the computer. Considering the focal distance and the cross sectional area of the transducer, the diameter of the focal spot was estimated to be 18μm at 80 MHz.

Analysis

The analysis for the pulse driven type microscopy is illustrated in Fig. 1 in comparison with the conventional burst driven type. The reflected wave is composed of the reflection at the front and rear surfaces of the tissue slice. In the pulse driven type, the reflected wave in the time domain is Fourier transformed into the frequency domain. Then the attenuation and phase spectra are compared with those of the direct reflection at the glass surface where no tissue is present. Because the signal is the result of the interference of two reflections, the attenuation spectrum has both maximum and minimum points as a function of frequency. Assuming $\int$m as one of the minimum and maximum points, and ϕm as the corresponding phase angle, the phase lag between the above two reflections at the minimum point is $(2n-1)\pi$, giving

$$2\pi f_m \times \frac{2d}{c_0} = \phi_m + (2n-1)\pi \quad (1),$$

where d, co, and n are the tissue thickness, sound speed of the water, and a non-negative integer, respectively. The phase lag at the maximum point is $2n\pi$, giving

$$2\pi f_m \times \frac{2d}{c_0} = \phi_m + 2n\pi \quad (2).$$

The phase angle ϕm can be expressed by

$$2\pi f_m \times 2d\left(\frac{1}{c_0} - \frac{1}{c}\right) = \phi_m \quad (3),$$

since ϕm is the phase lag between the wave passing through distance 2d with sound speed c and that passing though the corresponding distance with sound speed co. From eqs. (1) and (3),

$$d = \{\phi_m + (2n-1)\pi\} c_0 / 4\pi f_m \quad (4)$$

is obtained. The thickness d can also be obtained from eqs. (2) and (3) as

$$d = \{\phi_m + 2n\pi\} c_0 / 4\pi f_m \quad (5).$$

The sound speed is subsequently obtained as

$$c = \left(\frac{1}{c_0} - \frac{\phi_m}{4\pi f_m d}\right)^{-1} \quad (6).$$

After the measurement, staining with elastica van Gieson's stain was performed.

Real-time PCR

The specimens for total RNA extraction were conserved in RNAlater (Ambion, Austin, TX). Total RNA was isolated from human skin samples using TRIzol reagent (Invitrogen Life Technologies, Carlsbad, CA) and RNeasy Mini Kit (Qiagen, Valencia, CA). cDNA synthesis was carried out with MessageSensor™ RT Kit (Ambion). Real-time PCR was performed on the ABI PRISM 7000 Sequence Detection System (Applied Biosystems, Foster City, CA) using TaqMan Gene Expression probes and TaqMan Universal PCR Master Mix (Applied Biosystems). Gene-specific primers (Assay ID) were as follows: Type I collagen α1 subunit (COL1A1), Hs00164004; Type I collagen α2 subunit (COL1A2), Hs00164099; and tropoelastin (ELN), Hs00355783. The quantity of PCR products was calculated from the cycle threshold value. The levels of gene expression were normalized with those of the GAPDH gene.

Statistical analysis was performed using the Wilcoxon signed-rank test.

Immunohistochemical staining

Paraffin-embedded biopsies were sectioned (5μm), deparaffinized, ethanol-rehydrated, subjected to antigen retrieval, and rinsed with PBS. Nonspecific antibody binding was blocked by incubating the sections for 10 min in Protein Block Serum-Free (X0909, DAKO, Glostrup, Denmark). Blocked sections were incubated for 1 h with anti-collagen I (ab292, Abcam, Cambridge, UK) or anti-elastin (PR533, Elastin Products Company, MO, USA) in 1% BSA/PBS. The sections were then rinsed four times with PBS and incubated for 1 h with Fluorescein(FITC)-conjugated goat anti-rabbit IgG (111-095-144) or Cy3-conjugated goat anti-rabbit IgG (111-165-144, Jackson ImmunoResearch Laboratories, PA, USA). The slides were then sealed using SlowFade Antifade Kit (S-2828, Molecular Probes, OR, USA). The slides were examined by a laser scanning confocal microscope (Carl Zeiss LSM510, Jena, Germany).

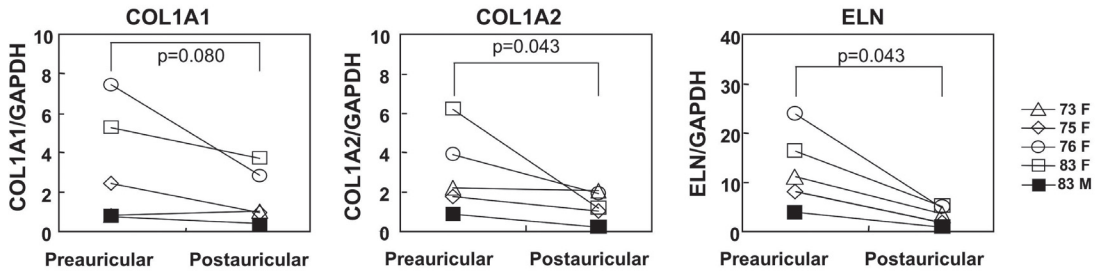

Fig. 2 Gene expression of procollagen and tropoelastin in the postauricular and preauricular skin. Total RNA were extracted from the postauricular and preauricular skin of the same subjects (n = 5), and applied to quantitative real-time PCR. Symbols shows age and sex of each subject. COL1A1, Type I collagen α1 subunit; COL1A2, Type I collagen α2 subunit; ELN, tropoelastin; GAPDG, glyceraldehydes-3-phosphate dehydrogenase

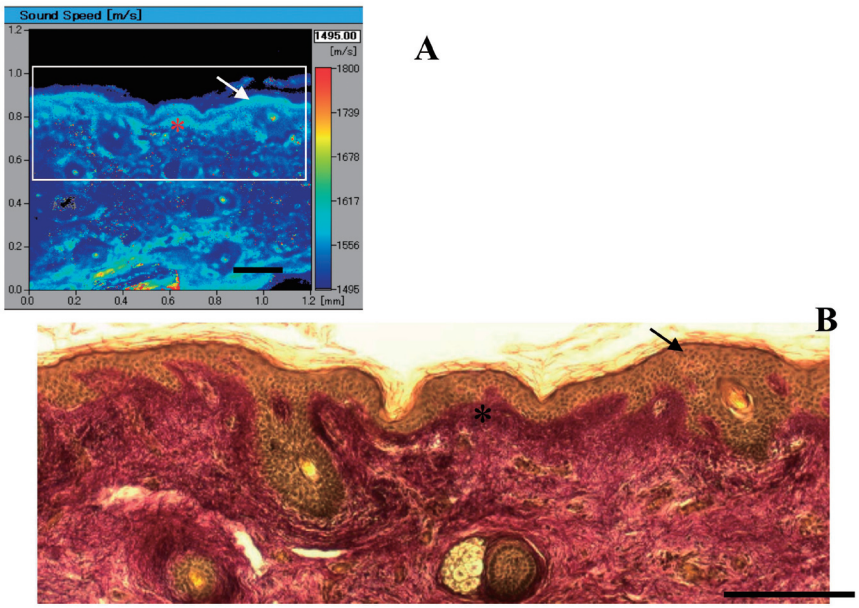

Fig. 3 Two-dimensional distribution of ultrasonic velocity and EVG staining of postauricular skin (66 year-old female). **A**, ultrasonic velocity; **B**, EVG stain. Higher ultrasonic velocity was observed in the uppermost of the stratum granulosum (arrow) and collagen layer beneath the epidermis (*).

RESULTS

To confirm the status of photodamage of aged preauricular skin, elastin and procollagen mRNA were measured by real-time PCR. The mRNA level of elastin in the preauricular skin was markedly increased compared with the postauricular skin (Fig. 2). Contrary to our expectations, the mRNA level of collagen α2 (I) in the preauricular skin was significantly increased and the mRNA level of collagen α1 (I) in the preauricular skin also tend to be increased, compared with the postauricular skin.

Figure 3 shows EVG staining and the acoustic image of postauricular skin (photo-protected area) of a female (66 years old). The sound speed varied from about 1500 to 1600 m/s in the tissue. The uppermost layer of keratinocytes and the dermis beneath the epidermis showed a relatively higher sound speed (light blue). The uppermost layer of keratinocytes seemed to coincide with the granular layer in the epidermis. The collagen

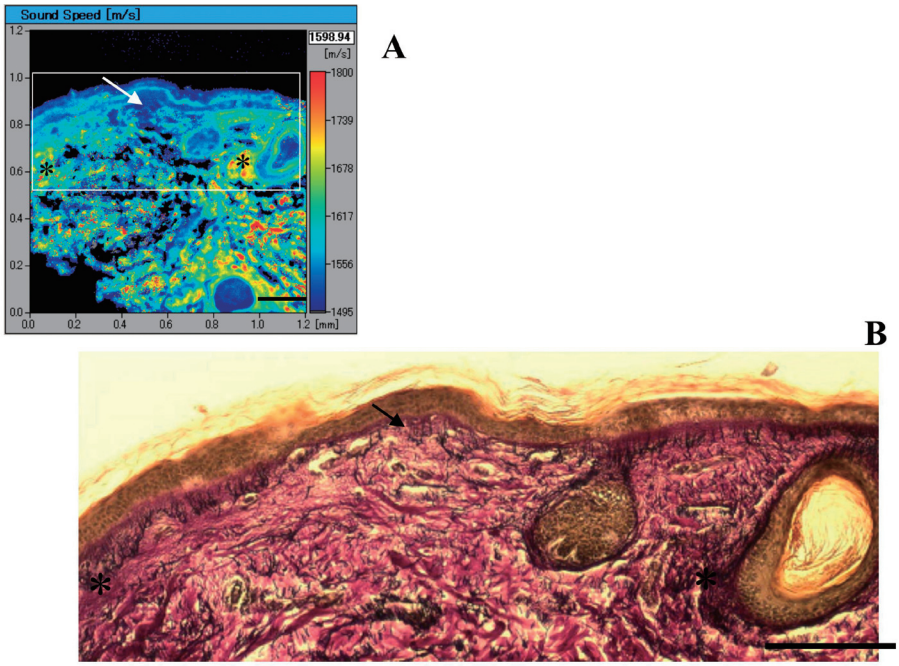

Fig. 4 Two-dimensional distribution of ultrasonic velocity and EVG staining of buttock skin. **A**, ultrasonic velocity; **B**, EVG stain. Decreased ultrasonic velocity was observed in the thin collagen layer beneath the epidermis (arrow). Higher ultrasonic velocity was observed in the dunning thick collagen fibers in the deeper dermis (*). Scale, 200μm

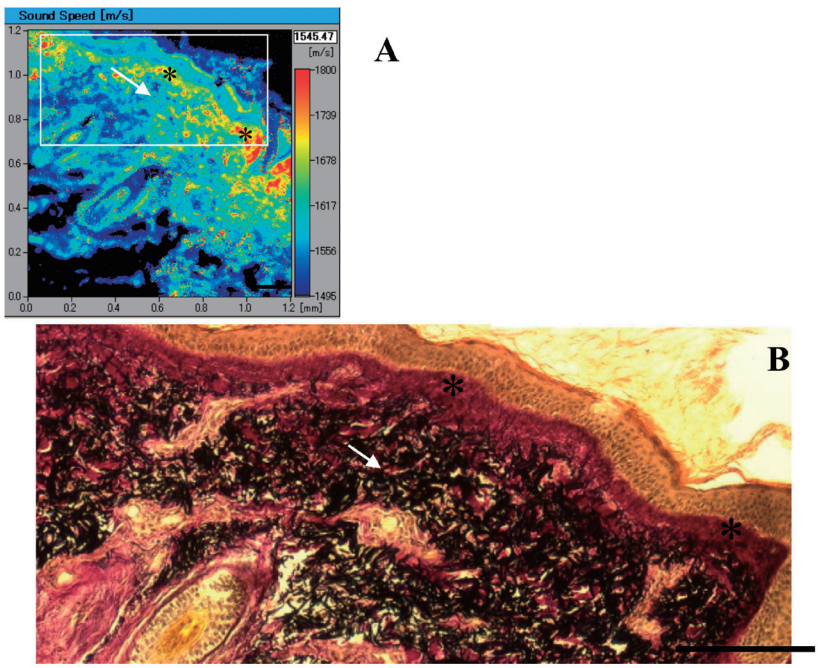

Fig. 5 Two-dimensional distribution of ultrasonic velocity and EVG staining of preauricular skin of subject shown in Fig. 3. **A**, ultrasonic velocity; **B**, EVG stain. Increased ultrasonic velocity in the Grenz zone (*) and decreased ultrasonic velocity in the solar elastosis were observed (arrow). Scale, 200μm

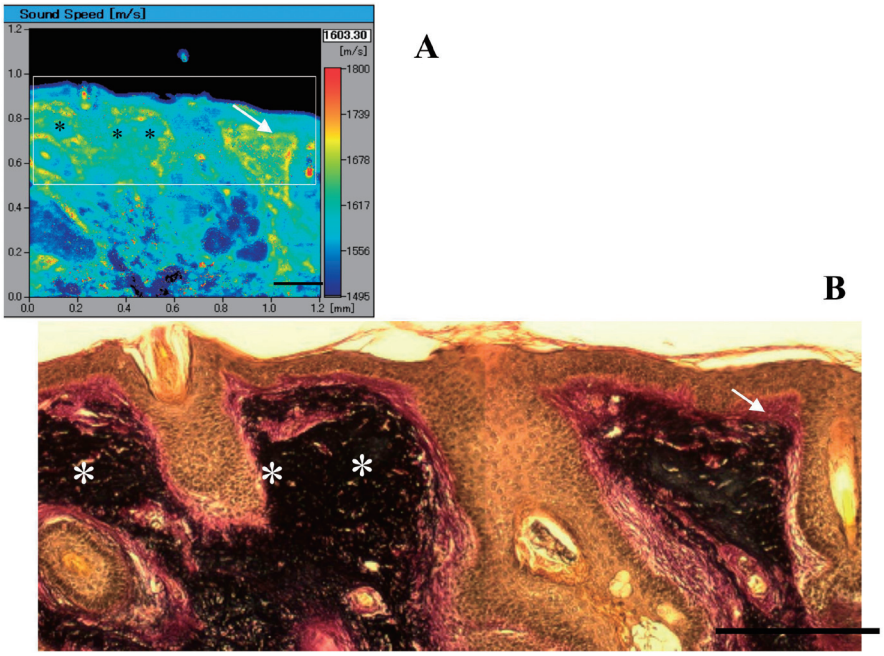

Fig. 6 Two-dimensional distribution of ultrasonic velocity and EVG staining of preauricular skin (69 year-old male). **A**, ultrasonic velocity; **B**, EVG stain. Increased ultrasonic velocity in the Grenz zone (arrow) and decreased ultrasonic velocity in part of the solar elastosis were observed (*). Scale, 200μm

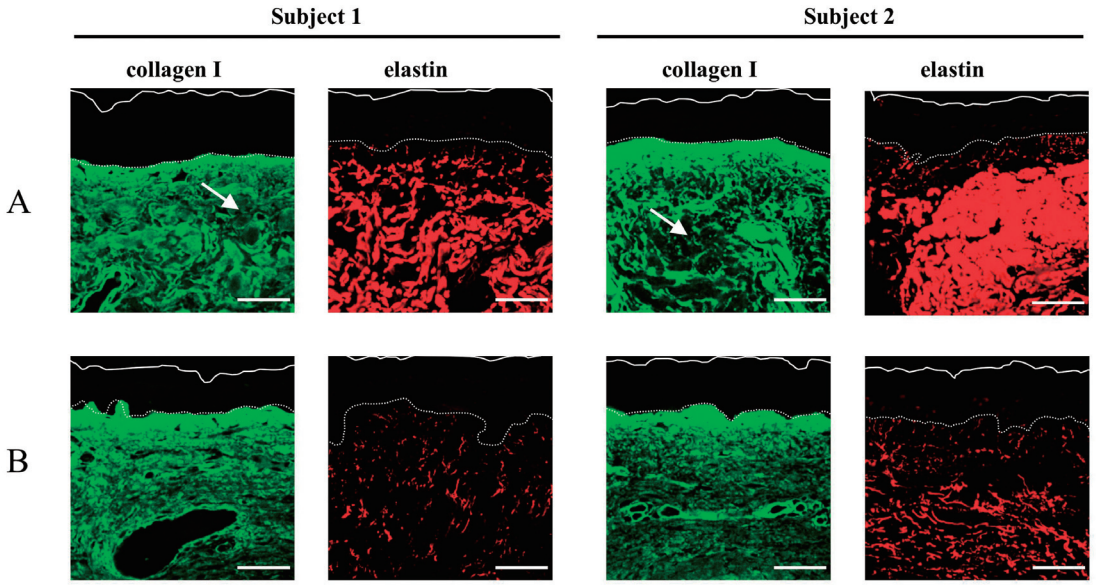

Fig. 7 Protein expression of procollagen and tropoelastin in postauricular and auricular skin. Preauricular (**A**) and postauricular skin (**B**) was obtained from subject 1 (shown in Fig. 3 and 5) and subject 2 (shown in Fig. 6). Procollagen (green) and tropoelastin (red) were stained immunohistochemically using corresponding antibodies. The dashed line shows the dermo-epidermal junction. The solid line shows the surface of the skin. Decreased signal (arrow) was observed at the site of solar elastosis. Scale, 100μm.

layer in the dermis beneath the epidermis had hardly any anchoring structure of oxytalan fibers as seen in the buttock skin (Fig. 3) but maintained an sound speed of about 1600 m/s, suggesting that the collagen layer sustained the physical strength of tissue. Figure 4 shows images of buttock skin (photo-protected area) of a female (69 years old). A decrease in sound speed was observed in the thin collagen layer without a progressive anchoring structure of oxytalan fibers. In the deeper dermis, higher sound speed (more than 1700 m/s) was observed in the thicker collagen fiber.

Figure 5 shows images of preauricular skin (photodamaged area) of a female (66 years old). The Grenz zone, which is a hallmark of photodamage, was developed on a clump of degenerated thick elastic fibers. The Grenz zone showed a higher sound speed (more than 1700 m/s). A decrease in the sound speed in part of the solar elastosis was observed. In the other case of preauricular skin (Fig. 6, 69 year-old male), solar elastosis was highly developed and the Grenz zone could be distinguished clearly by the sound speed (yellow to red).

To investigate the collagen content in the Grenz zone, skin samples were immunohistochemically stained using the antibody for collagen I. This antibody showed a stronger signal in the papillary dermis than in the deeper dermis both in the preauricular and postauricular skin (Fig. 7). The Grenz zone was clearly distinguished from the site of the deposition of elastin as seen by EVG staining in the preauricular skin. The Grenz zone conserved the signal of collagen I even in the more photodamaged preauricular skin (Fig. 7, subject 2). Deeper dermis showed a decreased signal of collagen I in part of the solar elastosis site.

DISCUSSION

In the present study, we first demonstrated the two-dimensional sound speed images of skin tissue at the microscopic level using scanning acoustic microscopy. We found four characteristic properties of sound speed in the skin as follows; (1) high sound speed of the keratinizing layer in the uppermost layer of the stratum granulosum, (2) discontinuous distribution of sound speed in the collagen layer beneath the epidermis in aged skin, (3) high sound speed associated with thick collagen fibers in the deeper dermis, and (4) an increase in the sound speed in the Grenz zone in photodamaged skin.

On the assumption that biological tissue is fluid-like, the sound speed is considered to be:

$$C = \sqrt{(K/\rho)} \quad (7).$$

where C is the sound speed, K is the elastic bulk modulus and ρ is the density. High molecular mass and highly elastic components in the skin increase the sound speed. Saijo *et al.* reported high sound speed associated with stiffness in fibrotic sites in the tissue of the infarcted myocardium. The sound speed is considered depend on the content and quality of collagen fibers [11]. In fact the intensity (dark pink color) of the EVG stain is almost coincident to with the sound speed in this study. Increased sound speed was associated with thicker collagen fiber in the deeper dermis of buttock skin.

The sound speed of the keratinizing layer on the uppermost layer of the stratum granulosum may reflect the condition of differentiation of keratinocytes because keratinocytes produce and cross-link with keratin and components of the cornified envelope in the terminal differentiation to corneocytes to produce rigid stratum corneum [13]. Cross-linking of the cornified envelope may be a polymerizing process influencing the sound speed. A discontinuous layer of sound speed is sometimes observed in the skin, suggesting the heterogeneous keratinizing state of the stratum corneum on the surface of the skin.

We choose postauricular skin as photo-protected skin. We confirmed markedly extremely increased expression of elastin gene in the preauricular skin, compared with the postauricular skin. Generally, buttock or forearm skin is often used as photo-protected skin in the study of photoaging. but there are few reports demonstrating a comparison between postauricular skin and preauricular skin. Bhawan *et al.* pointed structural differences between facial skin and forearm skin as photodamaged skin [1, 12]. When compared with buttock skin, postauricular skin has some differences as follows; (1) less anchoring structure of oxytalan fibers beneath the epidermis, (2) low content of elastic fibers and (3) a decrease in the sound speed in the dermis, suggesting that there

is a difference not only in the structure but also in physical properties. Disappearance of the anchoring structure of oxytalan fibers beneath the epidermis and decreased content of elastic fibers are the main changes in intrinsically aged skin [14]. The postauricular skin is reasonable as photo-protected skin compared with buttock skin.

Interestingly, in the postauricular skin, the papillary dermis showed a higher sound speed than that of deeper dermis. This zone is considered to be a site where newly synthesized collagen is localized [15, 16]. We also confirmed an intensive immunochemical signal of collagen I in the papillary dermis in the postauricular skin. This zone may have an important role in sustaining the strength of the skin. Alternately, the decrease in the sound speed was observed in the thin collagen layer without an anchoring structure of oxytalan fibers in the buttock skin, suggesting that the progression of oxytalan fiber may be related to the synthesis of collagen and the strength of collagen fibers.

Photodamaged skin shows hallmarks such Grenz zone formation and solar elastosis [17], but the physiological function of this zone has been not clarified. We first found that the Grenz zone showed a higher sound speed more than the site of solar elastosis, and that the sound speed in part of the solar elastosis was actually decreased. Moreover, we detected deposition of collagen I in the Grenz zone even in the more photodamaged preauricular skin. These results suggest that the fibrosis in the Grenz zone compensates the strength of tissue with the progress of solar elastosis. Photoaging brings a decreased elasticity of the skin. Ultraviolet rays are considered to promote the decrease in the collagen content [2], degeneration of collagen fibers [3], and accumulation of degenerated elastin [18]. In the Grenz zone, type I collagen synthesis is considered to be depressed in photodamaged skin [2, 16] and degenerated collagen fibers are observed [19, 20]. Type VII collagen synthesis is also reported to be depressed [21], although some reports demonstrate that the synthesis of type I collagen [22], type III collagen [23] and type VI collagen [24] is maintained in the Grenz zone. These discrepancies may be due to the status of photodamage and/or the examined site. We detected overall increased expression of collagen gene and conserved deposition of collagen I in the Grenz zone in the preauricular skin. Chung *et al*. also reported an increase in the collagen mRNA level in photoaged skin [22]. They argued that the degradation of collagen by MMPs was activated in the photodamaged skin. But localized modification of collagen may also take place in photodamaged skin. At least, the Grenz zone seems to exhibit different collagen metabolism than the the deeper dermis in photodamaged skin. Lavker emphasized that the Grenz zone, which had packed collagen fibrils in colinear arrangement, was a fibrosis-like microscar [17]. The Grenz zone may not be simply damaged, and rather plays an important role in sustaining the physical strength of photodamaged skin by rescuer fibrosis.

In conclusion, this study is the first to demonstrate the change of heterogeneous physical strength in the photodamaged skin using the SAM system. The SAM system will did in clarification of the role of structural proteins in photodamaged skin.

REFERENCES

1) Bhawan J, Andersen W, Lee J, Labadie R, Solares G. Photoaging versus intrinsic aging: a morphologic assessment of facial skin. J Cutan Pathol 1995; 22(2): 154-9.
2) Talwar HS, Griffiths CE, Fisher GJ, Hamilton TA, Voorhees JJ. Reduced type I and type III procollagens in photodamaged adult human skin. J Invest Dermatol 1995; 105(2): 285-90.
3) Nishimori Y, Edwards C, Pearse A, Matsumoto K, Kawai M, Marks R. Degenerative alterations of dermal collagen fiber bundles in photodamaged human skin and UV-irradiated hairless mouse skin: possible effect on decreasing skin mechanical properties and appearance of wrinkles. J Invest Dermatol 2001; 117(6): 1458-63.
4) Imokawa G, Takema Y, Yorimoto Y, Tsukahara K, Kawai M, Imayama S. Degree of ultraviolet-induced tortuosity of elastic fibers in rat skin is age dependent. J Invest Dermatol 1995; 105(2): 254-8.
5) Inomata S, Matsunaga Y, Amano S, Takada K, Kobayashi K, Tsunenaga M, *et al*. Possible involvement of gelatinases in basement membrane damage and wrinkle formation in chronically ultraviolet B-exposed hairless mouse. J Invest Dermatol 2003; 120(1): 128-34.
6) Cua AB, Wilhelm KP, Maibach HI. Elastic properties of human skin: relation to age, sex, and anatomical region. Arch Dermatol Res 1990; 282(5): 283-8.
7) Holbrook KA, Byers PH. Skin is a window on heritable disorders of connective tissue. Am J Med Genet 1989; 34(1): 105-21.
8) Ushiki T. Collagen fibers, reticular fibers and elastic fibers. A comprehensive understanding from a

morphological viewpoint. Arch Histol Cytol 2002; 65(2): 109-26.
9) Verdonk ED, Wickline SA, Miller JG. Anisotropy of ultrasonic velocity and elastic properties in normal human myocardium. J Acoust Soc Am 1992; 92(6): 3039-50.
10) Hoffmeister BK, Verdonk ED, Wickline SA, Miller JG. Effect of collagen on the anisotropy of quasi-longitudinal mode ultrasonic velocity in fibrous soft tissues: a comparison of fixed tendon and fixed myocardium. J Acoust Soc Am 1994; 96(4): 1957-64.
11) Saijo Y, Sasaki H, Naganuma T, Tanaka M. Ultrasonic tissue characterization of diseased myocardium by scanning acoustic microscopy. J Cardiol 1995; 25(3): 127-32.
12) Bhawan J, Oh CH, Lew R, Nehal KS, Labadie RR, Tsay A, *et al*. Histopathologic differences in the photoaging process in facial versus arm skin. Am J Dermatopathol 1992; 14(3): 224-30.
13) Nemes Z, Steinert PM. Bricks and mortar of the epidermal barrier. Exp Mol Med 1999; 31(1): 5-19.
14) Kligman AM, Zheng P, Lavker RM. The anatomy and pathogenesis of wrinkles. Br J Dermatol 1985; 113(1): 37-42.
15) Kligman LH. Effects of all-trans-retinoic acid on the dermis of hairless mice. J Am Acad Dermatol 1986; 15(4 Pt 2): 779-85, 884-7.
16) Nelson BR, Majmudar G, Griffiths CE, Gillard MO, Dixon AE, Tavakkol A, *et al*. Clinical improvement following dermabrasion of photoaged skin correlates with synthesis of collagen I. Arch Dermatol 1994; 130(9): 1136-42.
17) Lavker RM. Structural alterations in exposed and unexposed aged skin. J Invest Dermatol 1979; 73(1): 59-66.
18) Bernstein EF, Chen YQ, Tamai K, Shepley KJ, Resnik KS, Zhang H, *et al*. Enhanced elastin and fibrillin gene expression in chronically photodamaged skin. J Invest Dermatol 1994; 103(2): 182-6.
19) Bernstein EF, Chen YQ, Kopp JB, Fisher L, Brown DB, Hahn PJ, *et al*. Long-term sun exposure alters the collagen of the papillary dermis. Comparison of sun-protected and photoaged skin by northern analysis, immunohistochemical staining, and confocal laser scanning microscopy. J Am Acad Dermatol 1996; 34(2 Pt 1): 209-18.
20) Yamamoto O, Bhawan J, Solares G, Tsay AW, Gilchrest BA. Ultrastructural effects of topical tretinoin on dermo-epidermal junction and papillary dermis in photodamaged skin. A controlled study. Exp Dermatol 1995; 4(3): 146-54.
21) Craven NM, Watson RE, Jones CJ, Shuttleworth CA, Kielty CM, Griffiths CE. Clinical features of photodamaged human skin are associated with a reduction in collagen VII. Br J Dermatol 1997; 137(3): 344-50.
22) Chung JH, Seo JY, Choi HR, Lee MK, Youn CS, Rhie G, *et al*. Modulation of skin collagen metabolism in aged and photoaged human skin in vivo. J Invest Dermatol 2001; 117(5): 1218-24.
23) El-Domyati M, Attia S, Saleh F, Brown D, Birk DE, Gasparro F, *et al*. Intrinsic aging vs. photoaging: a comparative histopathological, immunohistochemical, and ultrastructural study of skin. Exp Dermatol 2002; 11(5): 398-405.
24) Watson RE, Ball SG, Craven NM, Boorsma J, East CL, Shuttleworth CA, *et al*. Distribution and expression of type VI collagen in photoaged skin. Br J Dermatol 2001; 144(4): 751-9.